Original article
DOI: https://doi.org/10.18721/JPM

THE LENGTH DISTRIBUTION OF NANOWIRES WITH FORWARD AND BACKWARD SURFACE DIFFUSION

V. G. Dubrovskii [1]✉, E. D. Leshchenko [2]

[1] St. Petersburg State University, St. Petersburg, Russia;
[2] Submicron Heterostructures for Microelectronics, Research & Engineering Center, RAS, St. Petersburg, Russia

✉dubrovskii.ioffe@mail.ru

Abstract. The length distributions of III – V nanowires growing by direct impingement and surface diffusion of adatoms are of fundamental and instrumentation interest. Here, we study kinetic rate equations for the length distribution of nanowires with forward and backward surface diffusion along their growing axes, where the average nanowire length either increases infinitely with time or saturates to a constant. We have obtained the exact solution to the discrete rate equations in the form of a modified Polya distribution, investigated its continuum approximation and analyzed the available experimental data on the length distributions of different III – V nanowires. The obtained results can be used to model various growth systems with size-linear forward and backward rate constants.

Keywords: nanowires, III–V semiconductors, length distribution, rate equations, modeling

Funding: Dubrovskii V. G. gratefully acknowledges financial support from the research grant of St. Petersburg State University (Grant No. 129360164).

For citation: Dubrovskii V. G., Leshchenko E. D., The length distribution of nanowires with forward and backward surface diffusion, St. Petersburg State Polytechnical University Journal. Physics and Mathematics. 18 (4) (2025) …–…. DOI: https://doi.org/10.18721/JPM.

Научная статья
УДК 538.975
DOI: https://doi.org/10.18721/JPM

РАСПРЕДЕЛЕНИЕ ПО ДЛИНАМ НИТЕВИДНЫХ НАНОКРИСТАЛЛОВ С ПОЛОЖИТЕЛЬНОЙ И ОТРИЦАТЕЛЬНОЙ ПОВЕРХНОСТНОЙ ДИФФУЗИЕЙ

В. Г. Дубровский [1]✉, Е. Д. Лещенко [2]

[1] Санкт-Петербургский государственный университет, Санкт-Петербург, Россия
[2] Научно-технологический центр микроэлектроники и субмикронных гетероструктур РАН, Санкт-Петербург, Россия

✉dubrovskii.ioffe@mail.ru

Аннотация. Распределения по длинам нитевидных нанокристаллов полупроводниковых соединений III – V групп представляют интерес с фундаментальной

точки зрения и для приборных приложений. В работе исследованы кинетические уравнения роста нитевидных нанокристаллов с положительной и отрицательной диффузией вдоль оси роста, с бесконечным ростом средней длины или ее насыщением на больших временных интервалах. Получено точное решение задачи в виде распределения Пойа, изучена континуальная форма данного распределения и проанализированы экспериментальные распределения по длине различных нитевидных нанокристаллов III – V групп. Полученные результаты можно использовать для моделирования различных систем, которые подчиняются уравнениям Беккера – Деринга с линейными по размеру константами скоростей роста и фрагментации.

Ключевые слова: нитевидный нанокристалл, полупроводниковые соединения III – V, распределение по длине, управляющие уравнения

Финансирование. Автор В. Г. Дубровский благодарит исследовательский грант Санкт-Петербургского государственного университета (грант № 129360164) за финансовую поддержку.

Для цитирования: Дубровский В. Г., Лещенко Е. Д. Распределение по длинам нитевидных нанокристаллов с положительной и отрицательной поверхностной диффузией // Научно-технические ведомости СПбГПУ. Физико-математические науки. 2025. Т. 18. № 4. С...–... . DOI: https://doi.org/10.18721/ JPM.

Introduction

Freestanding semiconductor nanowires (NWs), in particular III – V NWs and heterostructures of different types based on such NWs, are widely reported in the literature as promising building blocks for nanoscience and nanotechnology [1, 2]. These NWs are grown by the vapor-liquid-solid method with a foreign metal catalyst (often Au [3]), which can be replaced by a group III metal in the self-catalyzed vapor-liquid-solid approach [4], or via selective-area epitaxy without any catalyst [5]. Surface diffusion of group III adatoms contributes into the vertical growth rate of Au-catalyzed NWs preparing by the vapor-liquid-solid method, of catalyst-free NWs preparing by selective-area epitaxy procedure and of similar selective-area epitaxy structures such as elongated nanomembranes [6 – 12].

Surface diffusion along the NW sidewalls is also possible in the NWs of elemental semiconductors [6]. The total diffusion flux of group III adatoms to the NW top equals the forward (direct) flux minus the backward (rejected) one [6, 8, 9,

11, 12]. According to current concepts [11, 12], the backward diffusion flux depends on the nucleation-mediated growth rate on the top nanowire/nanomembrane facet and rapidly increases when the nucleation is suppressed by surface energetics or geometry (see Refs. [12, 13] and references therein). When adatoms are collected from the entire NW length and the total diffusion flux is positive, the NWs elongate exponentially with time [6, 8, 9, 12]. Negative diffusion flux leads to the limited growth regime with a length value saturation [12, 13].

Length distributions (LDs) of NWs are interesting from the fundamental viewpoint and paramount for processing and device functionalization of the NW ensembles. In particular, narrow length distributions enable easier contacting of as-grown NWs and suppress the unwanted inhomogeneous broadening of light-emitting devices [2].

Theoretical and experimental studies of the III – V NW length distributions [14 – 19] have led to the following results. NWs growing by the direct impingement without surface diffusion and nucleation delays feature the Poisson length distributions [14]. NWs growing by the direct impingement and forward diffusion from their entire length feature much broader Polya LDs [15]. Sub-Poissonian narrowing of the NW length distributions [18, 19] can be observed in thin enough NWs growing by the direct impingement due to a specific effect of nucleation antibunching which suppresses fluctuational broadenings [20 –24]. Nucleation delay in the formation of the very first NW monolayer above the substrate surface leads to a very significant broadening of the NW length distributions, with a long tail for shorter lengths [14, 16, 18]. It cannot be suppressed by nucleation antibunching [18]. Desorption of semiconductor material from a catalyst droplet does not change the Poisson shape of the length distributions [17].

On a more general ground, NWs growing by the direct impingement and surface diffusion present an interesting example of non-equilibrium system described by the Becker – Döring rate equations with size-linear rate constants, where the LDs can easily be measured in different growth stages. The Becker –

Döring rate equations are widely used in the nucleation theory [26 – 28] and other growth-related theories [29 – 52] including those for epitaxial islands [38 – 45]. One important outcome of these works in the Family – Vicsek scaling of the size distribution [38]. In Refs. [50 – 52], we demonstrated that size-linear forward rate constants naturally led to the Family – Vicsek scaling, which was confirmed experimentally for Au-catalyzed InAs NWs in Ref. [15]. However, backward surface diffusion was never studied in this regard.

Consequently, our goal of this work is to analyze theoretically the length distributions of nanowires with forward and backward diffusion and to reveal whether backward diffusion affects the previously obtained the Polya length distribution [15].

Computational model

The usual growth law for the length L of individual NW growing by the direct impingement from the vapor flux ν, forward and backward surface diffusion of adatoms is given by [6, 11, 12]:

$$\frac{dL}{dt} = \sigma\nu + \frac{2\lambda}{R}\tanh\left(\frac{L}{\lambda}\right)\eta\nu\left(1-c\right), \tag{1}$$

where λ is the diffusion length of adatoms on the NW sidewalls; σ, η are the dimensionless geometrical factors that depend on the droplet geometry (or the no droplet case for NWs grown through selective-area epitaxy and deposition technique (vapor deposition or directional molecular beam epitaxy); c is the factor for describing the backward diffusion (it is independent of the NW length).

The same growth law is valid for nanomembranes [12]. The case $c = 0$ corresponds to the absence of backward diffusion. Such a growth was earlier considered in Ref. [15]. For fairly short structures with $L << \lambda$, $\tanh(L/\lambda) = L/\lambda$. In this case, adatoms diffuse along the entire NW length and the NW growth rate scale linearly with L and is independent of λ [8, 9].

It is convenient to measure the NW length L in monolayers (MLs); this dimensionless length is

$$s = L/h = 0, 1, 2, \ldots,$$

where h is the height of a monolayer (in particular, h = 0.326 MLs for GaAs).

Introducing the dimensionless time τ and constant a according to expressions

$$\tau = \frac{2\eta\nu}{R}t,\ a = \frac{\sigma R}{2\eta h}, \tag{2}$$

Eq. (1) for the average NW length over the monolayers $\bar{s} = \langle s \rangle$ takes the following form:

$$\frac{d\bar{s}}{d\tau} = a + (1-c)\bar{s}. \tag{3}$$

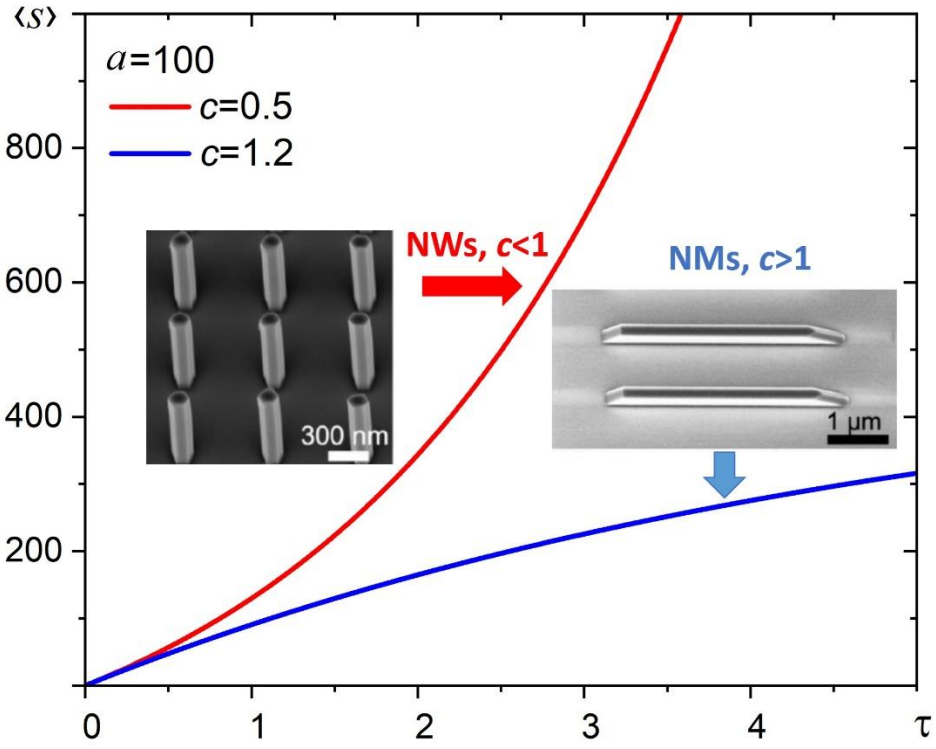

Fig. 1. A comparison of the curves' behavior of the average length ⟨s⟩ (over monolayers of NW) with dimensionless time τ for two c values at a = 100. *Inserts:* The examples of hexahedral GaAs NWs and elongated GaAs nanomembranes [10], exhibiting these growth regimes due to predominantly forward and backward surface Ga diffusion, respectively

The solution to Eq. (3) with zero initial condition at $\tau = 0$ is

$$\bar{s} = a\frac{e^{(1-c)\tau}-1}{1-c}. \tag{4}$$

From Eq. (4) it will be obvious that $\bar{s}$ increases infinitely at $c < 1$ and then saturates to the quantity

$$\bar{s}_{\infty} = a/(c-1) \text{ at } c > 1.$$

It can be seen from Fig. 1 an exponential growth of the average length at $c = 0.5$ and sublinear growth with the length saturation at $c = 1.2$ for $a = 100$. In so doing, the hexahedral GaAs NWs and elongated GaAs NMs from Ref. [10] exhibit superlinear and sublinear growth regimes due to predominantly forward and backward surface Ga diffusion, respectively (see inserts in Fig. 1). This explains the experimentally observed infinite and limited growth modes of nanowires and nanomembranes [11 – 13] but tells us nothing about the length distribution in the nanowire ensemble grown under identical conditions for each NW.

To access the statistical properties within the NW ensemble, we note that the NW formation occurs via the reaction scheme

$$A_sB + A_1 \leftrightarrow A_{s+1}B \text{ for } s = 0, 1, 2, \ldots,$$

where A_1 denotes the NW monolayer, and A_sB is the NW composed of s monolayers with $A_0B \equiv B$ as the nucleation seed (a catalyst nanoparticle for the vapor-liquid-solid growth or patterned pinhole in a mask layer for the selective-area epitaxy growth) [6,14 – 19].

We introduce the normalized length distribution $f_s(\tau)$ which satisfies the normalization condition

$$\sum_{s=0}^{\infty} f_s(\tau) = 1 \tag{5}$$

at any time.

The discrete set of the Becker – Döring rate equations for heterogeneous growth writes [6, 14 – 19, 50]:

$$\frac{df_0}{dt} = -J_1,$$
$$\frac{df_s}{dt} = J_s - J_{s+1}, s \geq 1. \quad (6)$$

The flux J_s for the regular growth rate given by Eq. (3) can be written as

$$J_s = (a+s) f_{s-1} - csf_s, s \geq 1. \quad (7)$$

The NW length distribution contains all statistical characteristics of a NW ensemble, including the average length $\bar{s}(\tau)$ and variance $D(\tau)$:

$$\bar{s}(\tau) = \langle s \rangle_\tau = \sum_{s=1}^{\infty} s f_s(\tau), D(\tau) = \left\langle (s - \bar{s})^2 \right\rangle_\tau = \langle s^2 \rangle_\tau - \bar{s}^2(\tau). \quad (8)$$

No nucleation delay for the formation of the very first NW monolayer is considered in this model. The nucleation delay is described by

$J_1 = bf_0 - cf_1$, with $b < a$ or even $b << a$ [14, 16, 18],

and strongly affects the length-distribution shape.

It was earlier considered for irreversible NW growth at $c = 0$ by the direct impingement without nucleation antibunching in Ref. [14], direct impingement with nucleation antibunching in Ref. [18], and direct impingement with forward surface diffusion of adatoms in Ref. [16]. Introduction of the nucleation delay in the Becker – Döring equations for reversible growth (at $c > 0$) is a very complex problem that will be studied elsewhere.

Analytic solution of the length distribution

Analytic solution of the Becker – Döring rate equations with size-linear rate constants is obtained by using the generating function for the length distributions [14 – 16, 50, 51]:

$$f(x, \tau) = \sum_{s=0}^{\infty} f_s(\tau) x^s. \quad (9)$$

Differentiating the generating function with respect to time and using Eqs. (6), we get

$$\frac{\partial f(x,\tau)}{\partial \tau} = \left(1 - \frac{1}{x}\right) \sum_{s=1}^{\infty} J_s(\tau) x^s. \tag{10}$$

Remarkably, size-linear rate constants yielding Eq. (7) for J_s lead to the closed first-order equation in partial derivatives for the generating function:

$$\frac{\partial f(x,\tau)}{\partial \tau} = (x-1)\left[(x-c)\frac{\partial f(x,\tau)}{\partial \tau} + af(x,\tau)\right]. \tag{11}$$

This equation should be solved with the initial condition

$$f(x, \tau = 0) = 1 \tag{12}$$

that corresponds to $f_0(\tau = 0) = 1$, $f_s(\tau = 0) = 0$ for $s \geq 1$ (no NWs at the beginning of deposition).

From Eq. (11), the generating function obeys the normalization condition $f(1,\tau) = 1$.

The average length is obtained from the equation

$$\bar{s}(\tau) = \left.\frac{\partial f(x,\tau)}{\partial x}\right|_{x=1}. \tag{13}$$

Differentiating Eq. (11) with respect to x and putting $x = 1$, we obtain Eq. (3) for the average length, with the solution given by Eq. (4). Now Eq. (11) contains only two parameters: a and c. Therefore, the resulting NW length distribution should be two-parametric. At $c = 0$, the solution should yield the result of Ref. [15], that is, the Polya length distributions for irreversible NW growth without backward diffusion.

Eq. (11) is solved by the method of characteristics. The equivalent system of ordinary differential equations is

$$\frac{d\tau}{1} = -\frac{dx}{(x-1)(x-c)} = \frac{df}{a(x-1)f}. \tag{14}$$

Integration of the first equation gives the first integral $T(x,\tau)$ of the form

$$e^{(1-c)(T-\tau)} = \frac{1-x}{c-x}. \tag{15}$$

Using the expression

$$x-1=(1-c)/\left\{\exp\left[(1-c)(\tau-T)\right]-1\right\}$$

in the second equation and integrating it with the initial condition

$$f(\tau=0)=1,$$

we obtain the following equation:

$$f(x,\tau)=\left[\frac{1-e^{(1-c)(T-\tau)}}{1-e^{(1-c)T}}\right]^{a}. \tag{16}$$

Using Eq. (15), the final result for the generating function is given by

$$f(x,\tau)=\frac{1}{\left[1+y(\tau)(1-x)\right]^{a}}, \tag{17}$$

with

$$y(\tau)=\frac{\bar{s}(\tau)}{a}=\frac{e^{(1-c)\tau}-1}{1-c}. \tag{18}$$

The discrete length distribution is obtained from this generating function by applying the known formulae:

$$\sum_{s=0}^{\infty}\frac{\Gamma(a+s)}{\Gamma(a)\Gamma(s+1)}\varepsilon^{s}=\frac{1}{(1-\varepsilon)^{a}},\varepsilon=\frac{y}{1+y}. \tag{19}$$

Our final result for the exact length distribution is given by the Polya distribution, which can be presented in the two equivalent forms:

$$\begin{aligned} f_s(\tau)&=\frac{1}{\left[1+y(\tau)\right]^{a}}\frac{\Gamma(a+s)}{\Gamma(a)\Gamma(s+1)}\left[\frac{y(\tau)}{1+y(\tau)}\right]^{s},s\geq 0,\\ f_s(\tau)&=\left[1+\frac{\bar{s}(\tau)}{a}\right]^{-a}\frac{\Gamma(a+s)}{\Gamma(a)\Gamma(s+1)}\left[1+\frac{a}{\bar{s}(\tau)}\right]^{-s},s\geq 0. \end{aligned} \tag{20}$$

Here Γ(ξ) denotes the gamma-function.

Results and discussion

Thus, the main result of this work can be formulated as follows. The nanowire length distribution in reversible growth with forward and backward surface diffusion of adatoms along their entire length is able to be given by the same Polya distribution as in Ref. [15] without backward diffusion.

However, there is one important difference. For irreversible growth at $c = 0$, the length distribution is truly one-parametric, because the average length of the Polya length distribution is given by the expression

$$\bar{s}(\tau) = a\left[\exp(\tau) - 1\right],$$

and increases infinitely in the large time limit.

Our refined model with arbitrary c describes either infinite growth at $c < 1$ or limited growth at $c > 1$, and hence is appropriate for a much wider range of data including the sub-linear growth regimes of nanowires and nanomembranes [6, 12, 13] as well as more general reversible growth systems [27 – 35]. In particular, the equilibrium length distribution at $c > 1$ is two-parametric:

$$f_s(\infty) = \left[1 - 1/c\right]^a \frac{\Gamma(a+s)}{\Gamma(a)\Gamma(s+1)} \frac{1}{c^s}, \tag{21}$$

with the average length $\bar{s}_\infty = a/(c-1)$.

This asymptotic equilibrium state is maintained even under the deposition flux due to the prevalent backward diffusion that equalizes the direct impingement flux and forward diffusion to the top of the structures.

The variance of the Polya length distribution is given by the expression

$$D = \frac{\bar{s}^2}{a} + \bar{s}. \tag{22}$$

Therefore, the asymptotic width $\sqrt{D}$ of the broad Polya length distribution is proportional to the average size at $\bar{s} \gg a$. At $a \to \infty$, the Polya length distribution is reduced to a much narrower Poisson one:

$$f_s(\bar{s}) = \exp(-\bar{s})\frac{\bar{s}^s}{s!}\bar{s}^s \cong \frac{1}{\sqrt{2\pi\bar{s}}}\exp\left[-\frac{(s-\bar{s})^2}{2\bar{s}}\right], \tag{23}$$

with the variance $D = \bar{s}$.

The continuum Polya LD at $s >> a$ is obtained in the same way as in Refs. [15, 50]. We use

$$(1+\bar{s}/a)^{-a} \cong (\bar{s}/a)^{-a}, \Gamma(a+s)/\Gamma(s+1) \cong s^{a-1},$$

along with

$$(1+a/\bar{s})^{-s} \cong \lim_{s\to\infty}\left[1+(as/\bar{s})/s\right]^{-s} = \exp(-as/\bar{s})$$

at large s and finite $as/\bar{s}$.

This results in the continuum LD has the form

$$f(s,\bar{s}) = \frac{1}{\bar{s}}\frac{a^a}{\Gamma(a)}\left(\frac{s}{\bar{s}}\right)^{a-1}\exp\left(-a\frac{s}{\bar{s}}\right). \tag{24}$$

From Eq. (2) in a, we can see that this parameter is always much larger than unity for NWs, ranging from about 10 for very thin NWs with $R \approx 5$ nm to ~200 nm for thicker NWs with $R \approx 50$ nm. At $a >> 1$, we can use the Stirling formula for

$$\Gamma(a) = \Gamma(a+1)/a = \sqrt{2\pi/a}\,(a/e)^a.$$

The function

$$x^{a-1}\exp(-ax) \cong \exp(-ax + a\ln x)$$

as the sharp maximum under the exponent at $x = 1$.

This allows us to write the following:

$$\exp\left(-ax+a\ln x\right)\cong\exp\left[-a-\left(a/2\right)\left(x-1\right)^2\right],$$

resulting in the symmetrical Gaussian approximation for the continuum length distribution [15]:

$$f\left(s,\bar{s}\right)=\frac{1}{\bar{s}}\sqrt{\frac{a}{2\pi}}\exp\left[-\frac{a}{2}\frac{\left(s-\bar{s}\right)^2}{\bar{s}^2}\right]. \tag{25}$$

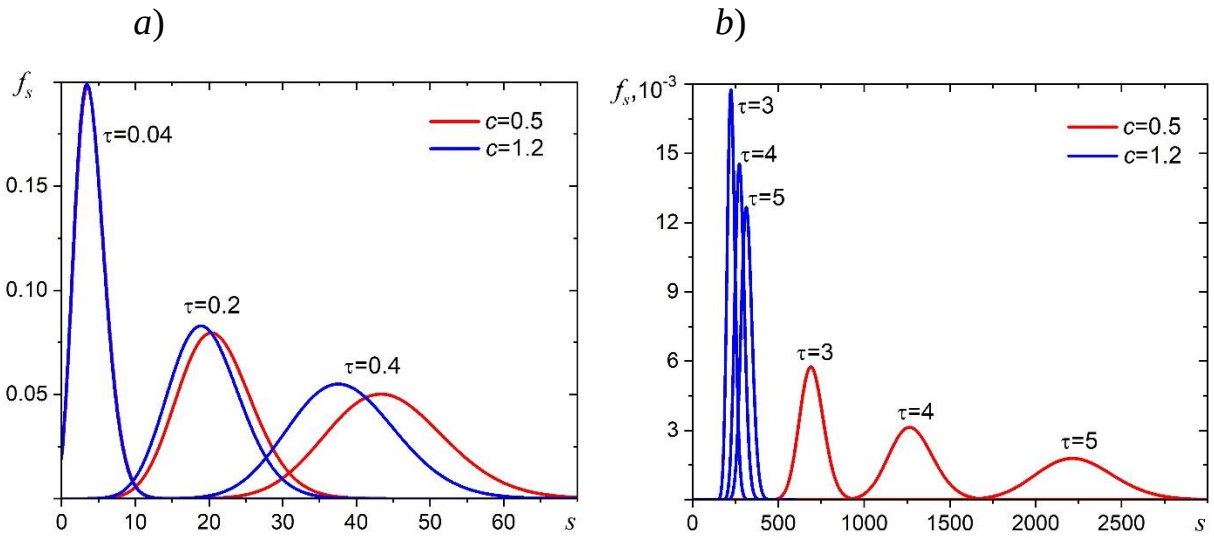

Fig. 2. Evolution of the NW length distributions in the initial growth stage (*a*) and for longer values of growth time τ: from 3 to 5 (*b*) in the infinite (c = 0.5) and limited (c = 1.2) growth regimes at a = 100; s is a number of NW monolayers

Fig. 2 shows the time evolution of the LD in the infinite (c = 0.5) and limited (c = 1.2) growth regimes with the same a value (a = 100). The LDs are similar in the initial stage for short τ values from zero to 0.4 (see Fig. 2,*a*), but become very different for longer growth times from 3 to 5 (see Fig. 2,*b*). These LDs are given by the same Eqs. (20). The only difference is in the average length $\bar{s}$, which is c-dependent and evolves differently in the infinite and limited growth regimes. Fig. 3 shows the equilibrium LDs given by Eq. (21) at different c values for the same a value (a = 10). These LDs narrow up for larger c, corresponding to the shorter equilibrium lengths.

Hence, the magnitude of the backward diffusion from top to bottom of the structures can be used as an additional tuning knob for their LDs.

It can be seen from Eq. (25) that the Family – Vicsek scaling function for the re-normalized LD $\bar{s}f\left(s,\bar{s}\right)$ versus $x=s/\bar{s}$ is given by the probability density of the gamma-distribution [16, 50]:

$$\bar{s}f\left(s,\bar{s}\right)=F\left(x\right)=\frac{a^a}{\Gamma\left(a\right)}x^{a-1}e^{-ax},x=\frac{s}{\bar{s}}. \tag{26}$$

At $a >> 1$ this is further reduced to

$$\bar{s}f\left(s,\bar{s}\right)=F\left(x\right)=\sqrt{\frac{a}{2\pi}}\exp\left[-\frac{a}{2}\left(x-1\right)^2\right]. \tag{27}$$

These universal scaling functions do not depend on the average NW length and satisfy the usual sum rules for the surface density and average size of the structures [38 – 44]:

$$\int_0^\infty dxF\left(x\right)=\int_0^\infty dxxF\left(x\right)=1. \tag{28}$$

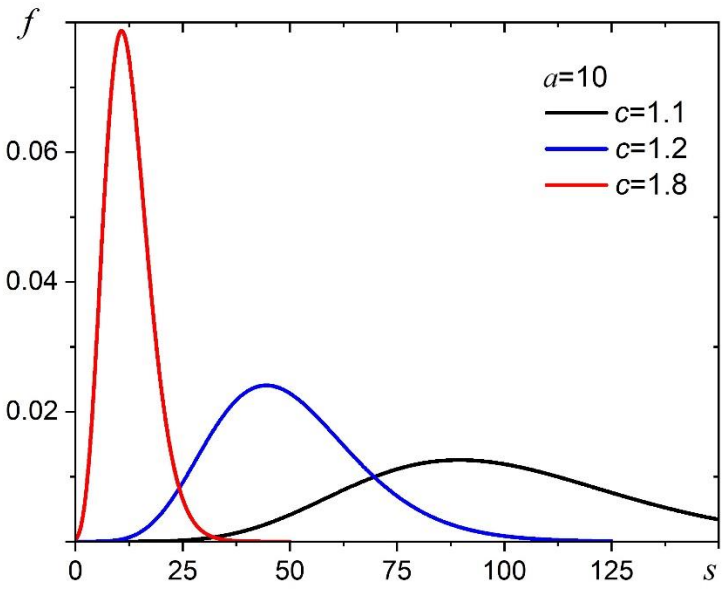

Fig. 3. Equilibrium NW length distributions at different c values (a = 10)

Fig. 3 shows the continuum length distributions given by Eqs. (24) and (26) in the natural and Family–Vicsek scaled variables at different a value from 1 to 250 for the same average length $\bar{s}$ = 3000. As mentioned above, the case a = 1 is not relevant for NWs, but may be interesting for other systems including linear rows of

metal adatoms on reconstructed Si surfaces [50, 53 – 55]. Generally, the Polya distribution is monotonically decreasing at $a \leq 1$ and unimodal at $a > 1$. The threshold case $a = 1$ corresponds to the geometrical distribution and the exponential Family–Vicsek scaling function $F(x) = \exp(-x)$. The Polya length distributions become more symmetric for larger a-values, with the Gaussian approximation becoming indistinguishable from Eqs. (24) or (26) at $a \geq 100$.

The shapes of both length distributions in Fig. 4 are similar. As evident, they narrow up for larger a-values.

However, the non-scaled length distributions in Fig. 3,*a* describe the NW ensemble with a given mean length, while the scaled length distributions in Fig. 3,*b* apply for any mean length $\bar{s} >> 1$ or, equivalently, for all but very short growth times.

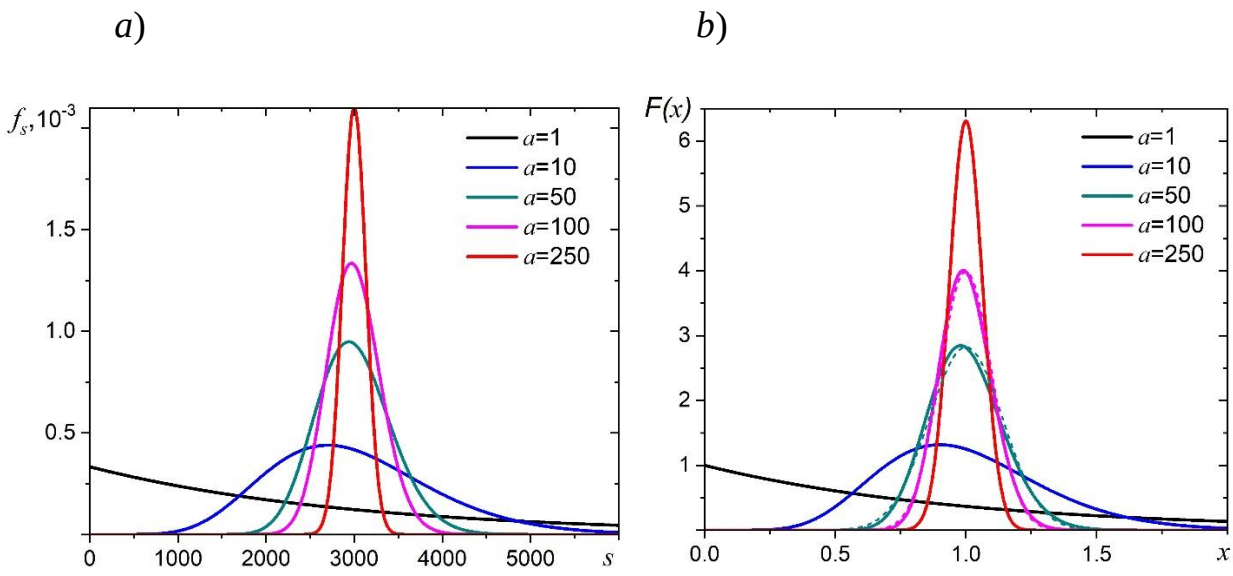

Fig. 4. Continuum LDs in the natural (*a*) and Family–Vicsek-scaled variables (*b*) for the same average length of 3000 monolayers and different a value.
In Fig. 4,*b*, the symmetrical Gaussian scaling function given by Eq. (27) is shown (dashed lines); it becomes indistinguishable from Eq. (26) at $a \geq 100$ for this average length

Fig. 5 shows the experimental NW length distributions with similar average lengths from Refs. [15, 19], fitted by the model. GaAs NWs of Ref. [19] were grown by the self-catalyzed vapor-liquid-solid method (with liquid Ga droplets). In this

case, the NW axial growth rate is controlled by the As input, and Ga surface diffusion does not contribute to the NW elongation. These LDs are well-fitted by the Poisson length distribution given by Eq. (23), with $\bar{s}$ = 4035 MLs and $D(\bar{s}) = \bar{s}$. InAs NWs of Ref. [15] were grown by the Au-catalyzed vapor-liquid-solid method, where indium surface diffusion is always effective. Consequently, their length distribution is well-fitted by the Polya distribution given by Eq. (27) with $\bar{s}$ = 4500 MLs and $D(\bar{s}) = \bar{s}^2/a$. This length distribution is much broader than Poissonian one. Further growth of these Ga-catalyzed GaAs NWs leads to sub-Poissonian narrowing due to nucleation antibuncning (as descrivbed in detail in Ref. [19]). No nucleation delays are prersent is both cases, which is achieved by the droplet organization prior to NW growth.

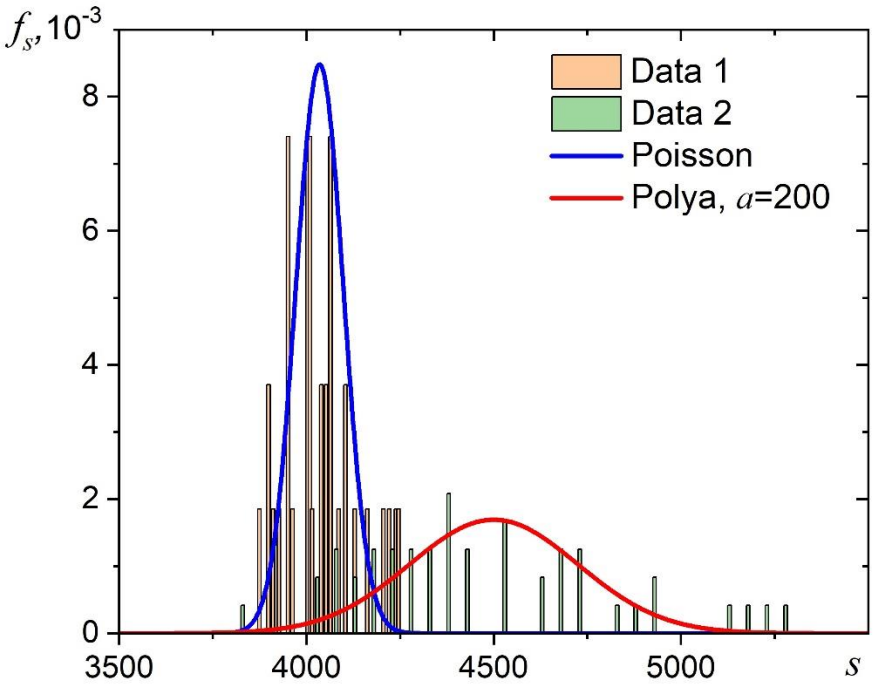

Fig. 5. LDs of self-catalyzed GaAs [19] (Data 1) and Au-catalyzed InAs [15] (Data 2) NWs with surface diffusion of group III adatoms with $\bar{s}$ = 4035 MLs and without it ($\bar{s}$ = 4500 MLs), respectively (histograms), fitted by the continuum Poisson (see Eq. (23)) and Polya LD with a = 200 (see Eq. (27)) (blue and red lines)

Summary

To summarize, it has been shown in the paper that backward diffusion of adatoms along the NW sidewalls does not obey the Polya LD shape, previously obtained for irreversible NW growth by surface diffusion [15, 16]. Consequently, the FV scaling form of the continuum LD remains the same. However, the reversible growth model describes different regimes of NW growth depending on the parameter c. At $c < 1$, NWs grow to infinite length, while at $c > 1$ they evolve to the equilibrium Polya distribution. These exact results can be used for understanding and controlling the NW/NM LDs grown by different epitaxy techniques and under different conditions, including the experimentally observed sublinear growth modes with the length saturation [11 – 13]. We hope that the obtained analytic distribution will be useful for modeling different systems including linear rows of adatoms [53 – 55], surface islands [26, 28, 37, 43, 44], planar NWs [56], and III – V ternary nanostructures [2]. The complex case of the diffusion-induced heterogeneous growth with a nucleation delay will be considered in our future work.

REFERENCES

1. **Ning C.-Z., Dou L., Yang P.,** Bandgap engineering in semiconductor alloy nanomaterials with widely tunable compositions, Nat. Rev. Mater. 2 (31 Oct) (2017) 17070.

2. **McIntyre P. C., Morral A. F. I.,** Semiconductor nanowires: To grow or not to grow? Mater. Today Nano. 9 (March) (2020) 100058.

3. **Wagner R. S., Ellis W. C.,** Vapor-liquid-solid mechanism of single crystal growth, Appl. Phys. Lett. 4 (5) (1964) 89–90.

4. **Colombo C., Spirkoska D., Frimmer M., et al.,** Ga-assisted catalyst-free growth mechanism of GaAs nanowires by molecular beam epitaxy, Phys. Rev. B. 77 (15) (2008) 155326.

5. **Aseev P., Fursina A., Boekhout F., et al.,** Selectivity map for molecular beam epitaxy of advanced III-V quantum nanowire networks, Nano Lett. 19 (1) (2019) 218–227.

6. **Dubrovskii V. G., Glas F.,** Vapor–liquid–solid growth of semiconductor nanowires, In book: N. Fukata, R. Rurali (Eds.), Fundamental properties of semiconductor nanowires, Springer Nature Pte Ltd., Singapore (2020) 1–38.

7. **Seifert W., Borgstrom M., Deppert K., et al.,** Growth of one-dimensional nanostructures in MOVPE, J. Cryst. Growth. 272 (1–4) (2004) 211–220.

8. **Plante M. C., LaPierre R. R.,** Analytical description of the metal-assisted growth of III–V nanowires: Axial and radial growths, J. Appl. Phys. 105 (11) (2009) 114304.

9. **Harmand J. C., Glas F., Patriarche G.,** Growth kinetics of a single $InP_{1-x}As_x$ nanowire, Phys. Rev. B. 81 (23) (2010) 235436.

10. **Mosiiets D., Genuist Y., Cibert J., et al.,** Dual-adatom diffusion-limited growth model for compound nanowires: Application to InAs nanowires, Cryst. Growth Des. 24 (9) (2024) 3888.

11. **Dubrovskii V. G.,** Nucleation-dependent surface diffusion in anisotropic growth of III–V nanostructures, Cryst. Growth Des. 24 (15) (2024) 6450.

12. **Zendrini M., Dubrovskii V., Rudra A., et al.,** Nucleation-limited kinetics of GaAs nanostructures grown by selective area epitaxy: Implications for shape engineering in optoelectronic devices, ACS Appl. Nano Mat. 7 (16) (2024) 19065–19074.

13. **Semlali E., Avit G., André Y., et al.,** Circumventing the ammonia-related growth suppression for obtaining regular GaN nanowires by HVPE, Nanotechnol. 35 (26) (2024) 265604.

14. **Dubrovskii V. G., Sibirev N. V., Berdnikov Y., et al.,** Length distributions of Au-catalyzed and In-catalyzed InAs nanowires, Nanotechnol. 27 (37) (2016) 375602.

15. **Dubrovskii V. G., Berdnikov Y., Schmidtbauer J., et al.,** Length distributions of nanowires growing by surface diffusion, Cryst. Growth Des. 16 (4) (2016) 2167–2172.

16. **Dubrovskii V. G.,** Length distributions of nanowires: Effects of surface diffusion versus nucleation delay, J. Cryst. Growth 463 (1 Apr) (2017) 139–144.

17. **Dubrovskii V. G., Barcus J., Kim W.,** Does desorption affect the length distributions of nanowires? Nanotechnol. 30 (47) (2019) 475604.

18. **Glas F., Dubrovskii V. G.,** Self-narrowing of size distributions of nanostructures by nucleation antibunching, Phys. Rev. Mater. 1 (3) (2017) 036003.

19. **Koivusalo E., Hakkarainen T., Guina M. T., Dubrovskii V. G.,** Sub-Poissonian narrowing of length distributions realized in Ga-catalyzed GaAs nanowires, Nano Lett. 17 (9) (2017) 5350–5355.

20. **Wen C.-Y., Tersoff J., Hillerich K., et al.,** Periodically changing morphology of the growth interface in Si, Ge, and GaP nanowires, Phys. Rev. Lett. 107 (2) (2011) 025503.

21. **Jacobsson D., Panciera F., Tersoff J., et al.,** Interface dynamics and crystal phase switching in GaAs nanowires, Nature. 531 (17 March) (2016) 317–322.

22. **Dubrovskii V. G.,** Refinement of nucleation theory for vapor – liquid – solid nanowires, Cryst. Growth Des. 17 (5) (2017) 2589–2593.

23. **Glas F., Panciera F., Harmand J. C.,** Statistics of nucleation and growth of single monolayers in nanowires: Towards a deterministic regime, Phys. Stat. Solidi (RRL). 16 (5) (2022) 2100647.

24. **Glas F.,** Incomplete monolayer regime and mixed regime of nanowire growth, Phys. Rev. Mater. 8 (4) (2024) 043401.

25. **Becker R., Döring W.,** Kinetische Behandlung der Keimbildung in übersättigten Dämpfern, Ann. Phys. 416 (8) (1935) 719–752.

26. **Kashchiev D.,** Nucleation: Basic theory with applications. Butterworth-Heinemann, Oxford, UK, 2000.

27. **Slezov V. V.,** Kinetics of first-order phase transitions, Wiley-VCH Verlag GmbH & Co., Berlin, 2009.

28. **Kukushkin S. A., Osipov A. V.,** Thin-film condensation processes, Phys. Usp. 41 (10) (1998) 983–l014.

29. **Ball J. M., Carr J., Penrose O.,** The Becker – Döring cluster equations: Basic properties and asymptotic behaviour of solutions, Commun. Math. Phys. 104 (4) (1986) 657–692.

30. **Jun Y.-S., Zhu Y, Wang Y., et al.,** Classical and nonclassical nucleation and growth mechanisms for nanoparticle formation, Annu. Rev. Phys. Chem. 73 (April) (2022) 453–477.

31. **Wattis J. A. D., King J. R.,** Asymptotic solutions of the Becker-Döring equations, J. Phys. A: Math. Gen. 31 (34) (1998) 7169.

32. **King J. R., Wattis J. A. D.,** Asymptotic solutions of the Becker–Döring equations with size-dependent rate constants, J. Phys. A: Math. Gen. 35 (6) (2002) 1357.

33. **Wattis J. A. D.,** A Becker-Döring model of competitive nucleation, J. Phys. A: Math. Gen. 32 (49) (1999) 8755.

34. **Wattis J. A. D.,** Similarity solutions of a Becker – Döring system with time-dependent monomer input, J. Phys. A: Math. Gen. 37 (32) (2004) 7823.

35. **Duncan D. B., Soheili A. R.,** Approximating the Becker – Döring cluster equations, Appl. Numer. Math. 37 (1–2) (2001) 1–29.

36. **Álvarez-Cuartas J. D., Camargo M., González-Cabrera D. L.,** Colloidal model for nucleation and aggregation in one dimension: Accessing the interaction parameters, Phys. Rev. E. 109 (6) (2024) 064604.

37. **Tomellini M., De Angelis M.,** Fokker-Planck equation for the crystal-size probability density in progressive nucleation and growth with application to lognormal, Gaussian and gamma distributions, J. Cryst. Growth. 650 (15 Jan) (2025) 127970.

38. **Vicsek T., Family F.,** Dynamic scaling for aggregation of clusters, Phys. Rev. Lett. 52 (19) (1984) 1669–1672.

39. **Bartelt M. C., Evans J. W.,** Exact island-size distributions for submonolayer deposition: Influence of correlations between island size and separation, Phys. Rev. B. 54 (24) (1996) R17359–R17362.

40. **Vvedensky D. D.,** Scaling functions for island-size distributions, Phys. Rev. B. 62 (23) (2000) 15435–15438.

41. **Körner M., Einax M., Maass P.,** Capture numbers and island size distributions in models of submonolayer surface growth, Phys. Rev. B. 86 (8) 085403.

42. **Evans J. W., Thiel P. A., Bartelt M. C.,** Morphological evolution during epitaxial thin film growth: Formation of 2D islands and 3D mounds, Surface Surf. Sci. Rep. 61 (1–2) (2006) 1–128.

43. **Dieterich W., Einax M., Maass P.,** Stochastic theories and scaling relations for early-stage surface growth, Eur. Phys. J. Spec. Top. 161 (1) (2008) 151–165.

44. **Einax M., Dieterich W., Maass P.,** Colloquium: Cluster growth on surfaces: Densities, size distributions, and morphologies, Rev. Mod. Phys. 85 (3) (2013) 921–939.

45. **Gibou F. G., Ratsch C., Caflisch R. E.,** Capture numbers in rate equations and scaling laws for epitaxial growth, Phys. Rev. B. 67 (15) (2003) 155403.

46. **Álvarez-Cuartas J. D., González-Cabrera D. L., Camargo M.,** Epitaxial growth in one dimension, J. Phys: Cond. Matter 36 (46) (2024) 463001.

47. **Aditya S., Roy N.,** Family-Vicsek dynamical scaling and Kardar-Parisi-Zhang-like superdiffusive growth of surface roughness in a driven one-dimensional quasiperiodic model, Phys. Rev. B. 109 (3) (2024) 035164.

48. **Bhakuni D. S., Lev Y. B.,** Dynamic scaling relation in quantum many-body systems, Phys. Rev. B. 110 (1) (2024) 014203.

49. **Fujimoto K., Hamazaki R., Kawaguchi Y.,** Family-Vicsek scaling of roughness growth in a strongly interacting Bose gas, Phys. Rev. Lett. 124 (21) (2020) 210604.

50. **Dubrovskii V. G., Berdnikov Yu. S.,** Natural scaling of size distributions in homogeneous and heterogeneous rate equations with size-linear capture rates, J. Chem. Phys. 142 (12) (2015) 124110.

51. **Dubrovskii V. G., Sibirev N. V.,** Analytic scaling function for island-size distributions, Phys. Rev. E. 91 (4) (2015) 042408.

52. **Dubrovskii V. G.,** A general solution to the continuum rate equation for island-size distributions: Epitaxial growth kinetics and scaling analysis, Nanomaterials. 15 (5) (2025) 396.

53. **Albao M. A., Evans M. M. R., Nogami J., et al.,** Monotonically decreasing size distributions for one-dimensional Ga rows on Si(100), Phys. Rev. B. 72 (3) (2005) 035426.

54. **Javorský J., Setvín M., Oštádal I., et al.,** Heterogeneous nucleation and adatom detachment at one-dimensional growth of In on Si (100)-2 × 1, Phys. Rev. B. 79 (16) (2009) 165424.

55. **Liu H., Reinke P.,** Formation of manganese nanostructures on the Si(100)-(2×1) surface, Surf. Sci. 602 (4) (2008) 986–992.

56. **Rothman A., Dubrovskii V. G., Joselevich E.,** Kinetics and mechanism of planar nanowire growth, Proc. Nat. Acad. Sci. USA. 117 (1) (2020) 152–160.

СПИСОК ЛИТЕРАТУРЫ

1. **Ning C.-Z., Dou L., Yang P.** Bandgap engineering in semiconductor alloy nanomaterials with widely tunable compositions // Nature Reviews Materials. 2017. Vol. 2. 31 October. P. 17070.

2. **McIntyre P. C., Morral A. F. I.** Semiconductor nanowires: To grow or not to grow? // Materials Today Nano. 2020. Vol. 9. March. P. 100058.

3. **Wagner R. S., Ellis W. C.** Vapor-liquid-solid mechanism of single crystal growth // Applied Physics Letters. 1964. Vol. 4. No. 5. Pp. 89 –90.

4. **Colombo C., Spirkoska D., Frimmer M., Abstreiter G., Morral A. F. I.** Ga-assisted catalyst-free growth mechanism of GaAs nanowires by molecular beam epitaxy // Physical Review B. 2008. Vol. 77. No. 15. P. 155326.

5. **Aseev P., Fursina A., Boekhout F., et al.** Selectivity map for molecular beam epitaxy of advanced III-V quantum nanowire networks // Nano Letters. 2019. Vol. 19. No. 1. Pp. 218–227.

6. **Dubrovskii V. G., Glas F.** Vapor–liquid–solid growth of semiconductor nanowires // N. Fukata, R. Rurali (Eds.) Fundamental properties of semiconductor nanowires. Singapore: Springer Nature Pte Ltd., 2020. Pp. 1–38.

7. **Seifert W., Borgstrom M., Deppert K., et al.** Growth of one-dimensional nanostructures in MOVPE // Journal of Crystal Growth. 2004. Vol. 272. No. 1–4. Pp. 211–220.

8. **Plante M. C., LaPierre R. R.** Analytical description of the metal-assisted growth of III–V nanowires: Axial and radial growths // Journal of Applied Physics.2009. Vol. 105. No. 11. P. 114304.

9. **Harmand J. C., Glas F., Patriarche G.** Growth kinetics of a single $InP_{1-x}As_x$ nanowire // Physical Review B. 2010. Vol. 81. No. 23. P. 235436.

10. **Mosiiets D., Genuist Y., Cibert J., Bellet-Amalric E., Hosevar M.** Dual-adatom diffusion-limited growth model for compound nanowires: Application to InAs nanowires // Crystal Growth Design. 2024. Vol. 24. No. 9. P. 3888.

11. **Dubrovskii V. G.** Nucleation-dependent surface diffusion in anisotropic growth of III–V nanostructures // Crystal Growth Design. 2024. Vol. 24. No. 15. P. 6450.

12. **Zendrini M., Dubrovskii V., Rudra A., Dede D., Morral A. F. I., Piazza V.** Nucleation-limited kinetics of GaAs nanostructures grown by selective area epitaxy: Implications for shape engineering in optoelectronic devices // ACS Applied Nano Materials. 2024. Vol. 7. No. 16. Pp. 19065–19074.

13. **Semlali E., Avit G., André Y., Gil E., Moskalenko A., Shields P., Dubrovskii V. G., Cattoni A., Harmand J.-Ch., Trassoudaine A.** Circumventing the ammonia-related growth suppression for obtaining regular GaN nanowires by HVPE // Nanotechnology. 2024. Vol. 35. No. 26. P. 265604.

14. **Dubrovskii V. G., Sibirev N. V., Berdnikov Y., Gomes U. P., Ercolani D., Zannier V., Sorba L.** Length distributions of Au-catalyzed and In-catalyzed InAs nanowires // Nanotechnology. 2016. Vol. 27. No. 37. P. 375602.

15. **Dubrovskii V. G., Berdnikov Y., Schmidtbauer J., Borg M., Storm K., Deppert K., Johansson J.** Length distributions of nanowires growing by surface diffusion // Crystal Growth Design. 2016. Vol. 16. No. 4. P. 2167–2172.

16. **Dubrovskii V. G.** Length distributions of nanowires: Effects of surface diffusion versus nucleation delay // Journal of Crystal Growth. 2017. Vol. 463. 1 April. Pp. 139–144.

17. **Dubrovskii V. G., Barcus J., Kim W.** Does desorption affect the length distributions of nanowires? // Nanotechnology. 2019. Vol. 30. No. 47. P. 475604.

18. **Glas F., Dubrovskii V. G.** Self-narrowing of size distributions of nanostructures by nucleation antibunching // Physical Review Materials. 2017. Vol. 1. No. 3. P. 036003.

19. **Koivusalo E., Hakkarainen T., Guina M. T., Dubrovskii V. G.** Sub-Poissonian narrowing of length distributions realized in Ga-catalyzed GaAs nanowires // Nano Letters. 2017. Vol. 17. No. 9. Pp. 5350–5355.

20. **Wen C.-Y., Tersoff J., Hillerich K., Reuter M. C., Park J. H., Kodambaka S., Stach E. A., Ross F. M.** Periodically changing morphology of the growth interface in Si, Ge, and GaP nanowires // Physical Review Letters. 2011. Vol. 107. No. 2. P. 025503.

21. **Jacobsson D., Panciera F., Tersoff J., Reuter M. C., Lechmann S., Hofmann S., Dick K. A., Ross F. M.** Interface dynamics and crystal phase switching in GaAs nanowires // Nature. 2016. Vol. 531. 17 March. Pp. 317–322.

22. **Dubrovskii V. G.** Refinement of nucleation theory for vapor–liquid–solid nanowires // Crystal Growth Design. 2017. Vol. 17. No. 5. Pp. 2589–2593.

23. **Glas F., Panciera F., Harmand J. C.** Statistics of nucleation and growth of single monolayers in nanowires: Towards a deterministic regime // Physica Status Solidi (RRL) – Rapid Research Letters. 2022. Vol. 16. No. 5. P. 2100647.

24. **Glas F.** Incomplete monolayer regime and mixed regime of nanowire growth // Physical Review Materials. 2024. Vol. 8. No. 4. P. 043401.

25. **Becker R., Döring W.** Kinetische Behandlung der Keimbildung in übersättigten Dämpfern // Annalen der Physik. 1935. Vol. 416. No. 8. Pp. 719–752.

26. **Kashchiev D.** Nucleation: Basic theory with applications. Oxford, UK: Butterworth-Heinemann, 2000. 544 p.

27. **Slezov V. V.** Kinetics of first-order phase transitions. Berlin: Wiley-VCH Verlag GmbH & Co., 2009. 415 p.

28. **Кукушкин С.А., Осипов А. В.** Процессы конденсации тонких пленок // Успехи физических наук. 1998. Т. 168. № 10. С. 1083–1116.

29. **Ball J. M., Carr J., Penrose O.** The Becker – Döring cluster equations: Basic properties and asymptotic behaviour of solutions // Communications in Mathematical Physics. 1986. Vol. 104. No. 4. Pp. 657–692.

30. **Jun Y.-S., Zhu Y, Wang Y., Ghim D., Wu X., Kim D., Jung H.** Classical and nonclassical nucleation and growth mechanisms for nanoparticle formation // Annual Review of Physical Chemistry. 2022. Vol. 73. April. Pp. 453–477.

31. **Wattis J. A. D., King J. R.** Asymptotic solutions of the Becker-Döring equations // Journal of Physics A: Mathematical and General. 1998. Vol. 31. No. 34. P. 7169.

32. **King J. R., Wattis J. A. D.** Asymptotic solutions of the Becker–Döring equations with size-dependent rate constants // Journal of Physics A: Mathematical and General. 2002. Vol. 35. No. 6. P. 1357.

33. **Wattis J. A. D.** A Becker-Döring model of competitive nucleation // Journal of Physics A: Mathematical and General. 1999. Vol. 32. No. 49. P. 8755.

34. **Wattis J. A. D.** Similarity solutions of a Becker – Döring system with time-dependent monomer input // Journal of Physics A: Mathematical and General. 2004. Vol. 37. No. 32. P. 7823.

35. **Duncan D. B., Soheili A. R.** Approximating the Becker – Döring cluster equations // Applied Numerical Mathematics. 2001. Vol. 37. No. 1–2. Pp. 1–29.

36. **Álvarez-Cuartas J. D., Camargo M., González-Cabrera D. L.** Colloidal model for nucleation and aggregation in one dimension: Accessing the interaction parameters // Physical Review E. 2024. Vol. 109. No. 6. P. 064604.

37. **Tomellini M., De Angelis M.** Fokker-Planck equation for the crystal-size probability density in progressive nucleation and growth with application to lognormal, Gaussian and gamma distributions // Journal of Crystal Growth. 2025. Vol. 650. 15 January. P. 127970.

38. **Vicsek T., Family F.** Dynamic scaling for aggregation of clusters // Physical Review Letters. 1984. Vol. 52. No. 19. Pp. 1669–1672.

39. **Bartelt M. C., Evans J. W.** Exact island-size distributions for submonolayer deposition: Influence of correlations between island size and separation // Physical Review B. 1996. Vol. 54. No. 24. Pp. R17359 – R17362.

40. **Vvedensky D. D.** Scaling functions for island-size distributions // Physical Review B. 2000. Vol. 62. No. 23. Pp. 15435–15438.

41. **Körner M., Einax M., Maass P.** Capture numbers and island size distributions in models of submonolayer surface growth // Physical Review B. 2012. Vol. 86. No. 8. Pp. 085403.

42. **Evans J. W., Thiel P. A., Bartelt M. C.** Morphological evolution during epitaxial thin film growth: Formation of 2D islands and 3D mounds // Surface Science Reports. 2006. Vol. 61. No. 1–2. Pp. 1–128.

43. **Dieterich W., Einax M., Maass P.** Stochastic theories and scaling relations for early-stage surface growth // The European Physical Journal. Special Topics. 2008. Vol. 161. No. 1. Pp. 151–165.

44. **Einax M., Dieterich W., Maass P.** Colloquium: Cluster growth on surfaces: Densities, size distributions, and morphologies // Reviews of Modern Physics. 2013. Vol. 85. No. 3. Pp. 921–939.

45. **Gibou F. G., Ratsch C., Caflisch R. E.** Capture numbers in rate equations and scaling laws for epitaxial growth // Physical Review B. 2003. Vol. 67. No. 15. Pp. 155403.

46. **Álvarez-Cuartas J. D., González-Cabrera D. L., Camargo M.** Epitaxial growth in one dimension // Journal of Physics: Condensed Matter. 2024. Vol. 36. No. 46. P. 463001.

47. **Aditya S., Roy N.** Family-Vicsek dynamical scaling and Kardar-Parisi-Zhang-like superdiffusive growth of surface roughness in a driven one-dimensional quasiperiodic model // Physical Review B. 2024. Vol. 109. No. 3. P. 035164.

48. **Bhakuni D. S., Lev Y. B.** Dynamic scaling relation in quantum many-body systems // Physical Review B. 2024. Vol. 110. No. 1. P. 014203.

49. **Fujimoto K., Hamazaki R., Kawaguchi Y.** Family-Vicsek scaling of roughness growth in a strongly interacting Bose gas // Physical Review Letters. 2020. Vol. 124. No. 21. P. 210604.

50. **Dubrovskii V. G., Berdnikov Yu. S.** Natural scaling of size distributions in homogeneous and heterogeneous rate equations with size-linear capture rates // The Journal of Chemical Physics. 2015. Vol. 142. No. 12. P. 124110.

51. **Dubrovskii V. G., Sibirev N. V.** Analytic scaling function for island-size distributions // Physical Review E. 2015. Vol. 91. No. 4. P. 042408.

52. **Dubrovskii V. G.** A general solution to the continuum rate equation for island-size distributions: Epitaxial growth kinetics and scaling analysis // Nanomaterials. 2025. Vol. 15. No. 5. P. 396.

53. **Albao M. A., Evans M. M. R., Nogami J., Zorn D., Gordon M. S., Evans J. W.** Monotonically decreasing size distributions for one-dimensional Ga rows on Si(100) // Physical Review B. 2005. Vol. 72. No. 3. P. 035426.

54. **Javorský J., Setvín M., Oštádal I., Sobotic P., Kotria M.** Heterogeneous nucleation and adatom detachment at one-dimensional growth of In on Si (100) -2 × 1 // Physical Review B. 2009. Vol. 79. No. 16. Pp. 165424.

55. **Liu H., Reinke P.** Formation of manganese nanostructures on the Si(100)-(2×1) surface // Surface Science. 2008. Vol. 602. No. 4. Pp. 986–992.

56. **Rothman A., Dubrovskii V. G., Joselevich E.** Kinetics and mechanism of planar nanowire growth // Proceedings of the National Academy of Sciences of the USA. 2020. Vol. 117. No. 1. Pp. 152–160.

THE AUTHORS

DUBROVSKII Vladimir G.
St. Petersburg State University
7 – 9 Universitetskaya Emb., St. Petersburg, 199034, Russia
dubrovskii.ioffe@mail.ru
ORCID: 0000-0003-2088-7158

LESHCHENKO Egor D.
Submicron Heterostructures for Microelectronics, Research & Engineering Center, RAS
26 Politekhnicheskaya St., St. Petersburg, 194021, Russia
leshchenko.spb@gmail.com
ORCID: 0000-0002-2158-9489

СВЕДЕНИЯ ОБ АВТОРАХ

ДУБРОВСКИЙ Владимир Германович – *доктор физико-математических наук, профессор кафедры физики твердого тела Санкт-Петербургского государственного университета, Санкт-Петербург, Россия.*
199034, Россия, г. Санкт-Петербург, Университетская наб., 7 – 9
dubrovskii.ioffe@mail.ru
ORCID: 0000-0003-2088-7158

ЛЕЩЕНКО Егор Дмитриевич – *кандидат физико-математических наук, младший научный сотрудник Научно-технологического центра микроэлектроники и субмикронных гетероструктур РАН, Санкт-Петербург, Россия.*
194021, Россия, г. Санкт-Петербург, Политехническая ул., 26
leshchenko.spb@gmail.com
ORCID: 0000-0002-2158-9489

Received 24.05.2025. Approved after reviewing 23.06.2025. Accepted 23.06.2025.
Статья поступила в редакцию 24.05.2025. Одобрена после рецензирования 23.06.2025. Принята 23.06.2025.